ANALYSIS OF CO-FLOW JET EFFECTS ON AIRFOIL AT MODERATE REYNOLDS NUMBERS

Abdolamir B. Khoshnevis, Shima Yazdani

Hakim Sabzevari University, Department of Mechanical Engineering, Sabzevar, Iran

e-mail: khoshnevis@hsu.ac.ir

Erfan Salimipour

Quchan University of Technology, Department of Mechanical Engineering, Quchan, Iran

This paper investigates the performance of controlling Co-Flow Jet (CFJ) on NACA 0025 airfoil at five different Reynolds numbers of $5 \cdot 10^4$, $7.5 \cdot 10^4$, 10^5, $1.5 \cdot 10^5$, and $3 \cdot 10^5$. To conduct the numerical solution of the fluid flow, 2D incompressible and unsteady Reynolds--averaged Navier-Stokes equations are solved using the SST-k-ω turbulence model. At all investigated Reynolds numbers, the lift coefficient enhances as the momentum coefficient increases, and its best performance is obtained at an angle of attack of (AoA) 15°. It is also observed that using the CFJ is of greater importance at $\text{Re} \leqslant 10^5$ than in other investigated cases.

Keywords: numerical solution, Co-Flow Jet (CFJ), stall, aerodynamic characteristics, momentum coefficient

1. Introduction

Investigating airfoil characteristics, particularly in incompressible low-Reynolds flows and changes in aerodynamic performance of the airfoils due to an increase in the Reynolds number is of paramount importance and has attracted many researchers. At low Reynolds numbers (usually lower than 200000), the flow tends to separate on the suction side, while it may reattach to the airfoil surface at higher Reynolds numbers. However, by decreasing the Reynolds number, this separated flow may not reattach to the airfoil surface due to the adverse pressure gradient (Yarusevych *et al.*, 2006). As the AoA increases, the vertical velocity and, consequently, the lift coefficient is increased. Furthermore, since the vertical velocity depends on the air resistance, the drag coefficient is also increased. This trend continues up to a specific angle, called the stall angle. When stall happens, devastating effects on aerodynamic performance occur; the lift coefficient dramatically decreases while the drag coefficient continues to increase. Therefore, the flying object can fly no more. Thus, applying methods to control the stall phenomenon and control the separation flow is of great importance. The airfoil aerodynamic performance can be enhanced with adequate energy and momentum transported to the boundary layer using flow control methods in order to reach desired aerodynamic goals including delaying the transition, delaying the separation, and improving the aerodynamic efficiency. As the flow separation occurs, a substantial reduction and a considerable increase are produced in the lift and drag coefficients, respectively. Various flow control methods have been presented so far (Salimipour and Yazdani, 2015, 2020; Salimipour *et al.*, 2016; Jansen *et al.*, 2017; Shokrgozar Abbasi and Yazdani, 2019). Implementing the flow control and avoiding the separation occurrence, a thin boundary layer remains which prevents from the pressure drop at the trailing edge and, as a result, reduces the drag to reach its minimum. The co-flow jet (CFJ) is a relatively modern active flow control method which was proposed by Zha and Paxton (2004) for the first time.

Using injection and suction in the CFJ airfoil with resistance against the adverse pressure gradient causes the main-flow to be attached particularly at high angles of attack. A suction slot contributes to reaching the net jet mass flow rate zero. Zha and Gao (2006) experimentally investigated the effects of CFJ on NACA 0025 airfoil at the Reynolds number of $3.8 \cdot 10^5$. They used a thin wire at the front of the airfoil to induce the flow turbulence and investigated a number of different momentum coefficients (pressure ratio). Their results indicated that the airfoil with CFJ had the maximum lift of 2.2 times greater than that for the baseline airfoil. They replicated their experiments using numerical methods, where there was a good agreement between the results for the lift coefficient. However, the stall AoA was predicted by numerical method 3° higher than its experimental value. Wells *et al.* (2006) conducted some experiments to investigate the effect of the injection slot size on the lift coefficient, drag coefficient and stall angle. To that end, experiments were carried out for two different sizes of the injection slot of 0.0065 and 0.013 times the airfoil chord length for the airfoil NACA 0025. For the same angle of attack, their results revealed that the airfoil with a smaller injection slot had a better performance of increasing the stall angle and maximum lift. However, the airfoil with a larger injection slot had a more enhanced performance of reducing the drag. Therefore, to obtain the same lift, an airfoil with a smaller injection slot consumes lower energy than an airfoil with a larger injection slot. In order to examine the effect of suction on the performance of CFJ airfoil, Zha *et al.* (2007) simulated two NACA 0025 airfoils at the same Reynolds number of $3.8 \cdot 10^5$ and with the same injection slot of 0.0065 times the wing cord where one airfoil had a suction slot of 0.0196 times the wing chord length and with the other without the suction slot. This study showed that the suction slot on the suction side of the CFJ airfoil offered a better performance compared to the mode with only injection where the suction was supplied by the engine intake. Their numerical results demonstrated that the lift coefficient and stall AoA increased for both the airfoils such that the airfoil without the suction slot stalled at the angle of 39° while the other airfoil experienced it at the angle of 43°. Dano *et al.* (2010, 2011) experimentally studied the performance of CFJ for an airfoil fabricated at Miami University for three different momentum coefficients, and explained the reasons for lift enhancement, drag reduction and an increase in the stall angle. Abinav *et al.* (2016) in a numerical study performed comparison of the performance of NACA 6409 baseline airfoil and the CFJ airfoil with varying positions of injection and suction slots. Zhang *et al.* (2018a,b) conducted a numerical study to explore the effects of CFJ on NACA 0012 airfoil with a flap. They obtained the optimum flap length and investigated the effects of CFJ at a few momentum coefficients and calculated their corresponding aerodynamic performances. Lefebvre *et al.* (2016) conducted an experimental and numerical study to assess the effects of CFJ on NACA6415 airfoil for a range of the Mach number from 0.03 to 0.4 at a constant momentum coefficient of 0.8 and for an AoA range of 0° and 30°. Their results showed that as the Mach number increased due to compressibility effects, the maximum lift coefficient increased. Up to the Mach number of 0.3, there were negligible variations in the drag, and the pressure coefficient was reduced. However, at the Mach number of 0.4, the drag and pressure coefficients drastically increased due to the emergence of shock and a substantial increase in the entropy. Furthermore, other studies have been conducted on the effects of CFJ on a cylinder, wing and airfoil (Hossain *et al.*, 2015; Mirhosseini and Khoshnevis, 2016; Lefebvre *et al.*, 2016; Ethiraj, 2017; Zhang *et al.*, 2018a,b; Yang and Zha, 2018a,b; Satyajit and Rathakrishnan, 2018; Ren and Zha, 2018).

In the present study, we simulate a 2D flow to investigate the effects of CFJ on NACA 0025 airfoil based on the Reynolds number increment. This investigation is carried out at five different Reynolds numbers of $5 \cdot 10^4$, $7.5 \cdot 10^4$, 10^5, $1.5 \cdot 10^5$, and $3 \cdot 10^5$ and four different momentum coefficients of 0.03, 0.06, 0.09, and 0.13 for an AoA range of 0°-20°. The present paper is aimed at evaluating the CFJ performance by changing the Reynolds number and jet

momentum coefficient and comparing all the states with the baseline airfoil. Moreover, the optimum value of the momentum coefficient is also calculated at each angle.

2. Mathematical and numerical formulation

In this Section, the numerical procedure used to compute the unsteady, viscous and incompressible flow is described.

2.1. Governing equations

The integral formulations for mass and momentum conservation are represented as follows

$$\oint_{\partial \Omega} \rho V \, dS = 0 \qquad \frac{\partial}{\partial \tau} \int_{\Omega} \mathbf{W} \, d\Omega + \oint_{\partial \Omega} \mathbf{J} \, dS = 0 \qquad (2.1)$$

where Ω is the control volume bounded by the closed surface $\partial \Omega$, ρ is the fluid density, V denotes the contravariant velocity defined as the velocity normal to the surface element dS, $\mathbf{W}$ is the vector of the so-called conservative variables and $\mathbf{J}$ denotes the sum of convection and diffusion fluxes expressed as

$$\mathbf{W} = \begin{bmatrix} \rho u \\ \rho v \end{bmatrix} \qquad \mathbf{J} = \begin{bmatrix} \rho u V + n_x p - (\mu + \mu_t)\left(n_x \frac{\partial u}{\partial x} + n_y \frac{\partial u}{\partial y}\right) \\ \rho v V + n_y p - (\mu + \mu_t)\left(n_x \frac{\partial v}{\partial x} + n_y \frac{\partial v}{\partial y}\right) \end{bmatrix} \qquad (2.2)$$

$$V \equiv \mathbf{v} \cdot \mathbf{n} = n_x u + n_y v$$

with n_x and n_y being the components of the outward facing unit normal vector of the surface $\partial \Omega$, μ and μ_t are the laminar and turbulent viscosity, respectively. Also, the SST-k-ω model is used to simulate the turbulent flow.

2.2. Mesh generation and boundary conditions

In this paper, CFJ is constructed at the suction surface of the baseline NACA 0025 airfoil to produce a jet tangential to the main-flow. The applied computational domain is depicted in Fig. 1. To solve the flow solution, a C-type structured grid is used. Figure 2 shows the applied
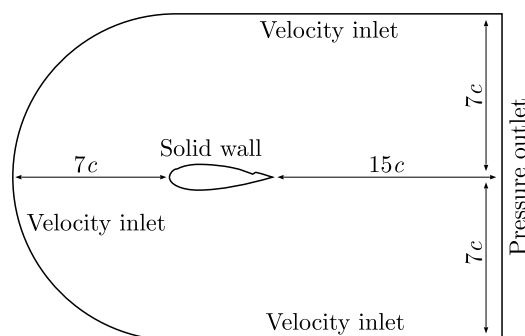

Fig. 1. Computational domain and applied boundary conditions around the NACA 0025 airfoil

mesh to solve the flow. As it can be observed, the nodes possess an appropriate perpendicular to one another. To investigate grid independency of the computational domain, meshes with different numbers of cells are evaluated, and their results are compared with each other. Figure 3 shows a comparison between the results of meshes with 578×61, 601×71, and 626×71 nodes for the CFJ airfoil velocity profile with a momentum coefficient of 0.05 for the angle of 5° and at the Reynolds number of 10^5, at a distance of 0.47 times the chord length from the leading edge. The mesh with 626×71 node is selected for the conducted computations.
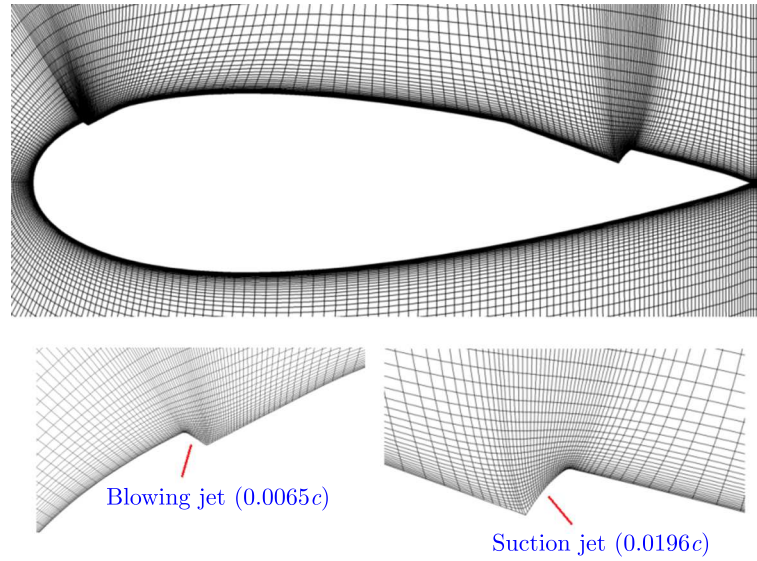
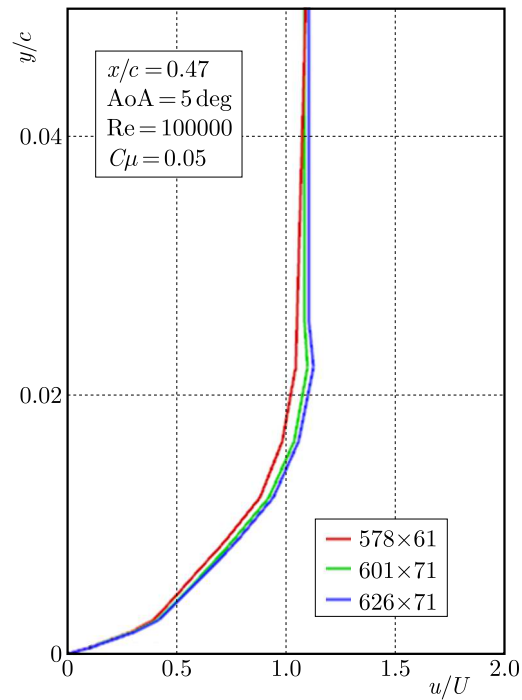Fig. 2. The grid used in flow computations and location of the CFJ on the airfoil

Fig. 3. Comparison of the velocity profile for different computational grids

3. Results and discussion

3.1. Code validation study

Before using the present solver to analyze the problem, it is necessary to test the validity of the flow solver. Experimental data obtained by Zha *et al.* (2006) were used to evaluate solver ability for the configuration NACA 0025 and CFJ0025-65-196 at the Reynolds number of $3.8 \cdot 10^5$. Figure 4 depicts the results of this comparison. As it can be observed that there is an acceptable agreement between numerical and experimental results.
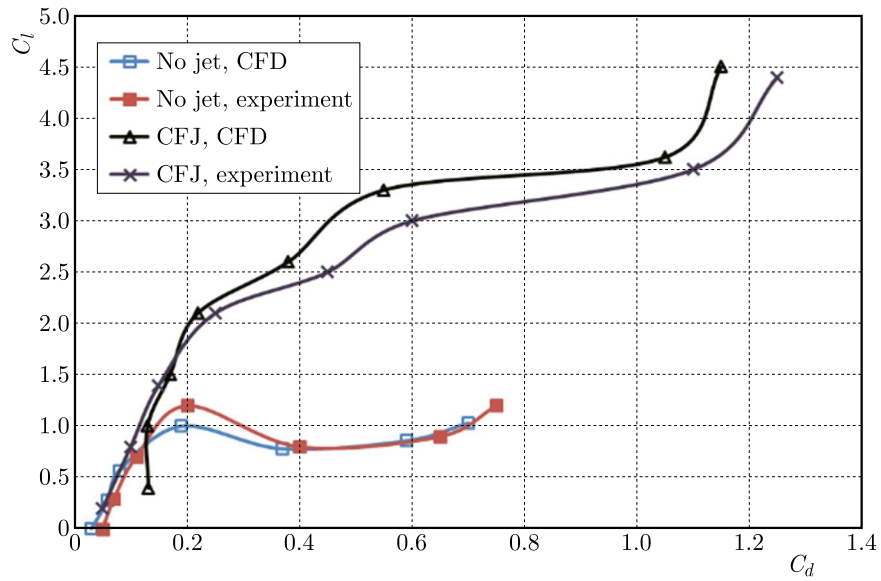
Fig. 4. Comparison of drag polar for the present solver and experimental data (Zha *et al.*, 2006)
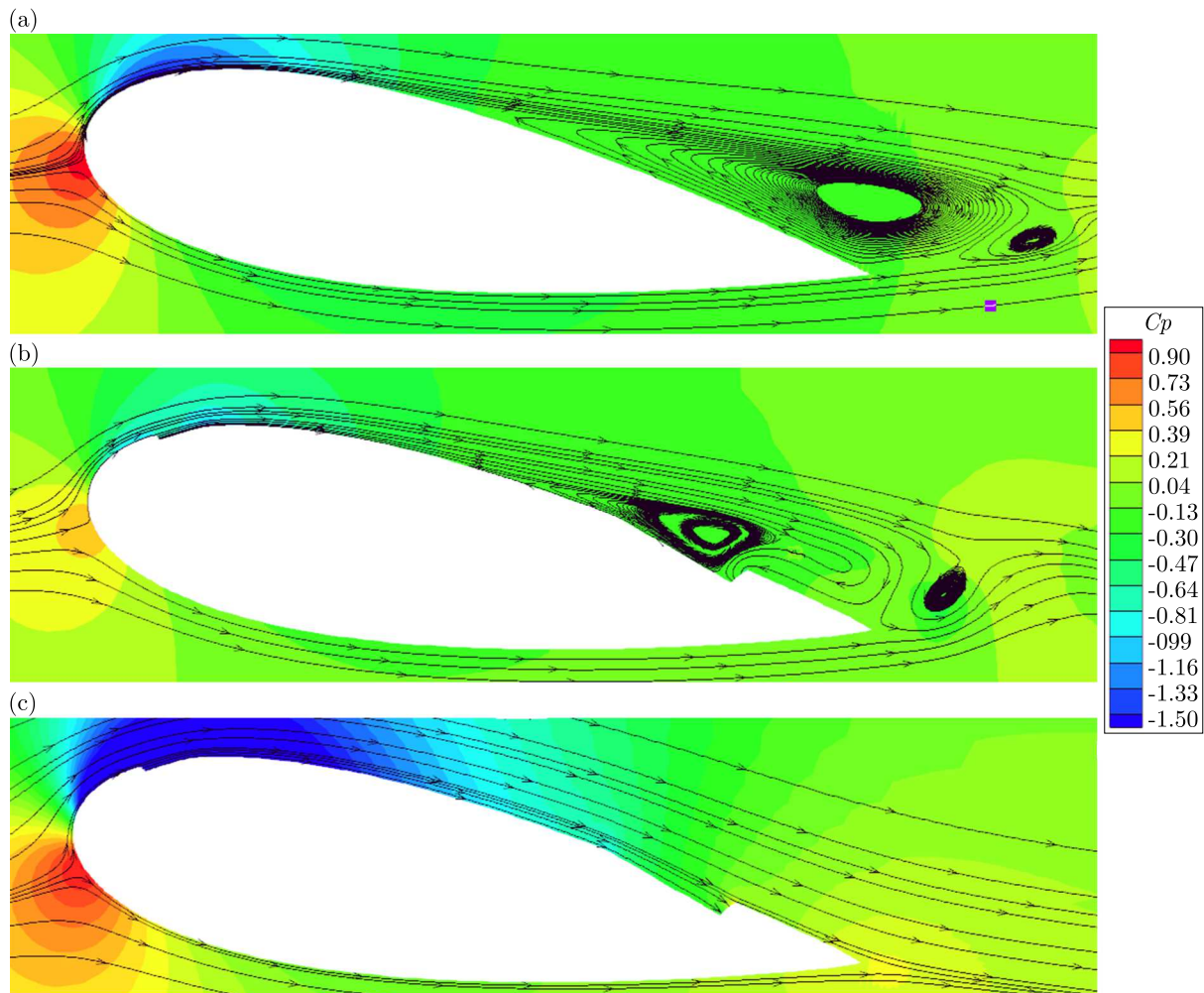

Fig. 5. Effects of CFJ on streamlines and pressure coefficient contours for AoA = 10° at Re = 10^5: (a) baseline airfoil, (b) CFJ_Cμ = 0.03, (c) CFJ_Cμ = 0.06
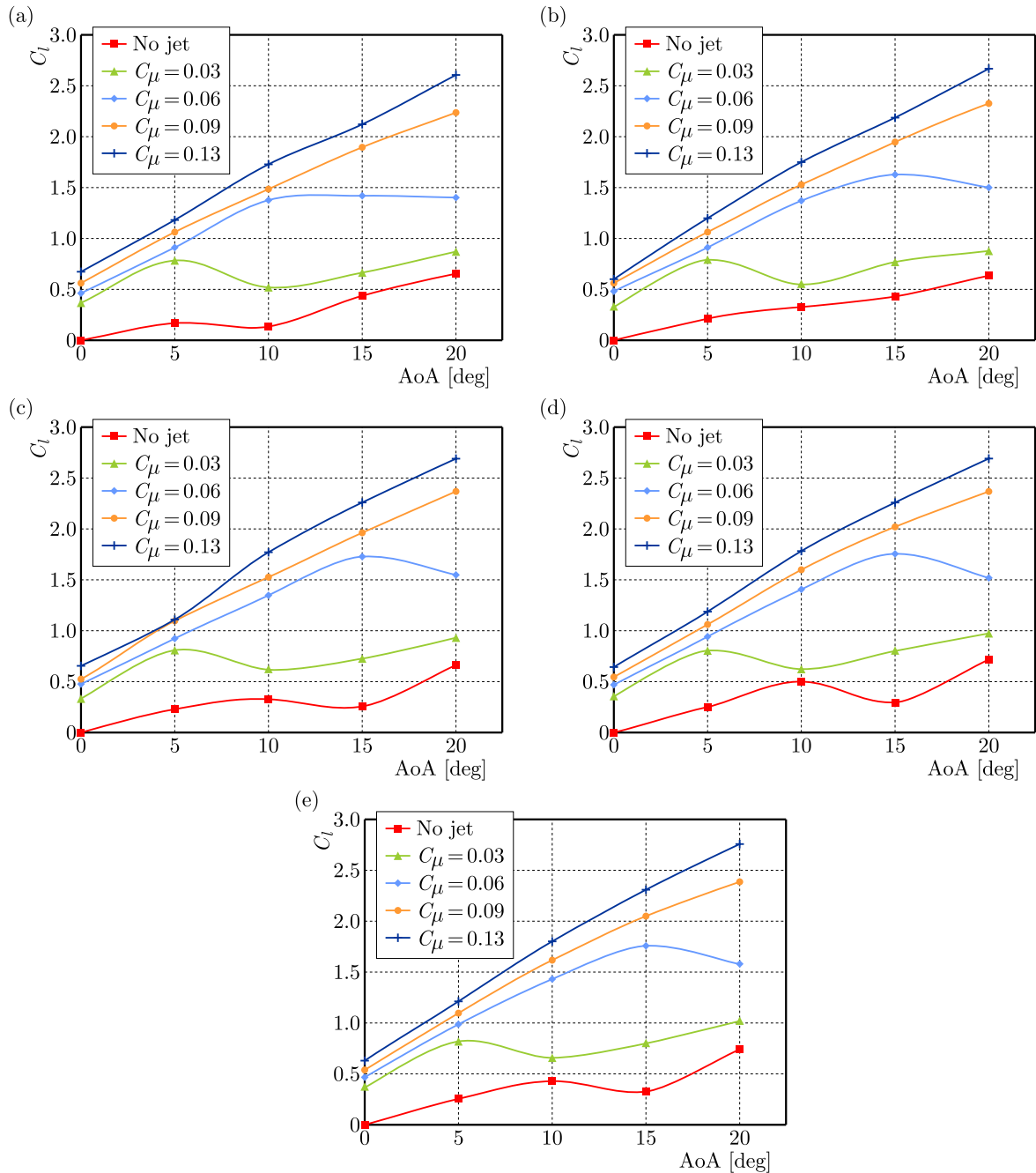
Fig. 6. Comparison of lift coefficients between the baseline airfoil and the CFJ with different $C\mu$ levels at (a) $\mathrm{Re} = 5 \cdot 10^4$, (b) $\mathrm{Re} = 7.5 \cdot 10^4$, (c) $\mathrm{Re} = 10^5$, (d) $\mathrm{Re} = 1.5 \cdot 10^5$, (e) $\mathrm{Re} = 3 \cdot 10^5$

3.2. Evaluation of CFJ performance on aerodynamic coefficients

By implementing the CFJ on NACA 0025 airfoil, the performance of this active control method on aerodynamic coefficients is assessed at five Reynolds numbers. This evaluation is carried out for different jet momentum coefficients of 0.03, 0.06, 0.09, and 0.13 in an AoA range of 0°-20°.

Figure 5 illustrates contours of the pressure coefficient and streamlines at the angle of 10° for both the baseline and CFJ airfoils at the Reynolds number of 10^5 with two momentum coefficients of 0.03 and 0.06. As it can be observed, a large vortex is created at the trailing edge of the baseline airfoil. Once the flow is separated, an increase in the momentum coefficient of

the CFJ causes an increase in the turbulence of the injection jet mixing zone. By increasing the momentum of the flow, which is created due to applying CFJ with the momentum coefficient of 0.03, the separation is delayed to some extent and the vortex decreases in size. By increasing the momentum coefficient to 0.06, the required energy remains the boundary layer attached, and thus the separation is eliminated.

Figure 6 shows the lift coefficient for the baseline airfoil and CFJ airfoil at five investigated Reynolds numbers with various momentum coefficients. Regarding the fact that stall occurs at lower angles of attack for smaller momentum coefficients, the lift coefficient first increases and then decreases after a specific angle. By increasing the momentum coefficient due to delaying the stall angle, this lift reduction is observed in a higher AoA. These phenomena can be seen in Figs. 6-8. They are associated with the lift coefficient at different Reynolds numbers. That is to say, according to Fig. 6a, that lift reduction occurs at the angle of 5° for the momentum coefficient of 0.03 that is identical to that for the baseline airfoil while it occurs at the angle of 15° for the momentum coefficient of 0.06. For higher values of momentum coefficients in the angle range investigated in this paper, there is no occurrence of stall, and the lift coefficient does not decrease. According to Figs. 6b-6e, similar behavior for the lift coefficient can be observed at other Reynolds numbers.

By increasing the lift coefficient at higher angles of attack, due to vertical velocity increase, the drag coefficient also grows. According to Fig. 7 which illustrates changes in the drag coefficient at different Reynolds numbers, the difference of the drag coefficient between the CFJ airfoil and the baseline airfoil is large at first implying that applying CFJ at small angles of attack causes a significant increase in the drag coefficient. As the angle of attack increases, the drag coefficient experiences a descending trend such that it reaches a lower value at the angle of 20° than that for the baseline airfoil. Furthermore, it can be observed in the diagrams that at all Reynolds numbers and for most of the angles, the drag coefficient increases as the momentum coefficient reaches 0.09. However, for the momentum coefficient of 0.13, it reaches a value lower than that for the momentum coefficient of 0.06.

To better understand the effects of the CFJ, we investigate the effect of flow control over the lift to drag ratio. Figure 8 depicts the lift to drag ratio at different Reynolds numbers. The performances of the CFJ airfoil show its sensitivity depending on momentum coefficients and Reynolds numbers, for which and for any angle of attack an optimum momentum coefficient is achieved. To get a better comparison, Table 1 is prepared to give the optimum momentum coefficient for each angle at the investigated Reynolds numbers. The results reveal that for small angles of attack before the occurrence of stall, a small moment coefficient leads to higher efficiency and better performance of the airfoil, while high values of the momentum coefficient produce inappropriate results. Therefore, there is a maximum value of the jet momentum coefficient which when exceeded decreases the system performance. As it can be observed in Table 1, at all investigated Reynolds numbers, the optimum value of the momentum coefficient is obtained at 0.03 for angles of attack of 0° and 5° while various amounts are obtained at angles of attack of 10°-20°.

Table 1. Optimal momentum coefficient at each angle of attack

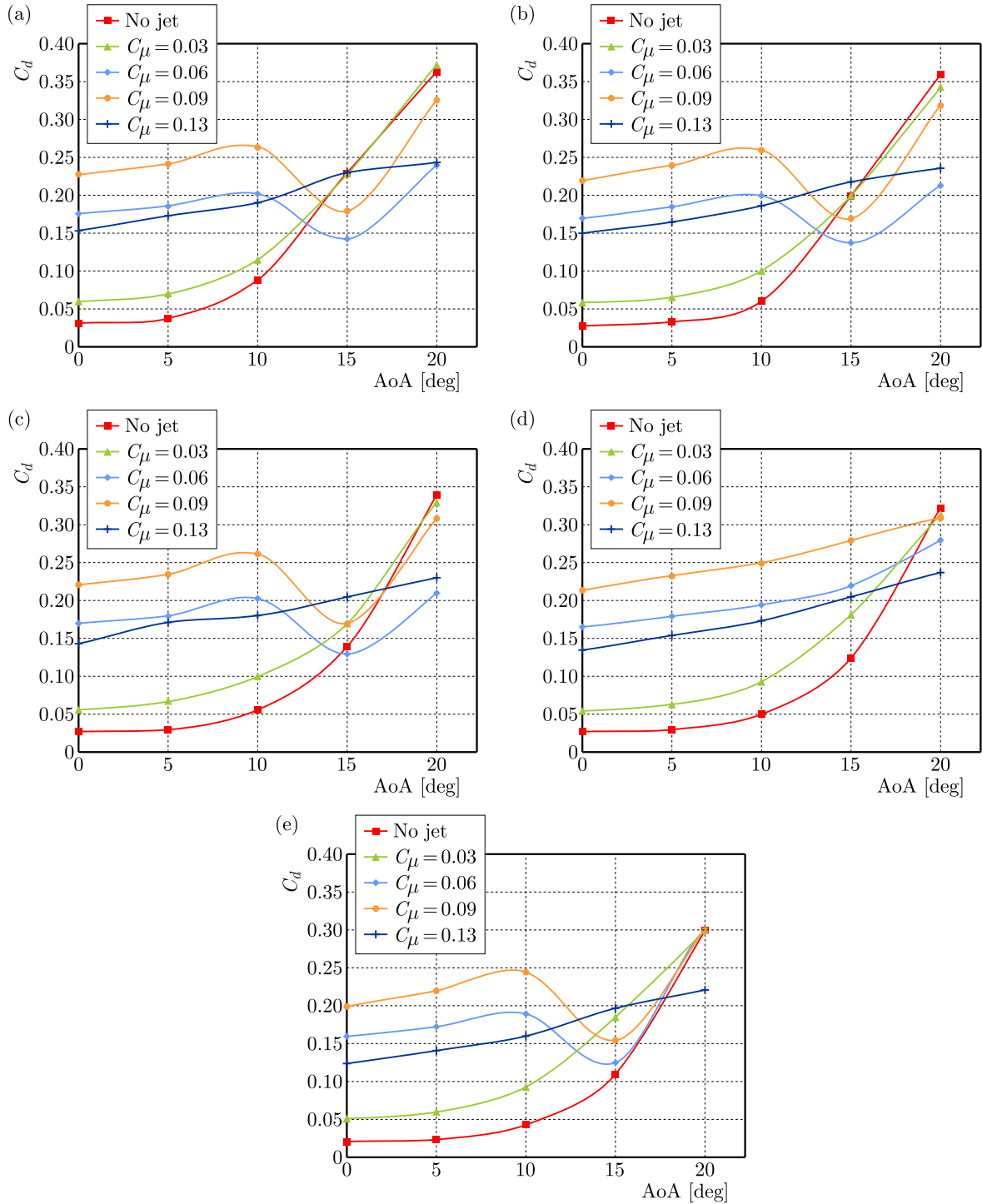| AoA [deg]	Re = $5 \cdot 10^4$		Re = $7.5 \cdot 10^4$		Re = 10^5		Re = $1.5 \cdot 10^5$		Re = $3 \cdot 10^5$	
	$C\mu$	C_l/C_d	$C\mu$	C_l/C_d	$C\mu$	C_l/C_d	$C\mu$	C_l/C_d	$C\mu$	C_l/C_d
0	0.03	6.03	0.03	5.69	0.03	5.9	0.03	6.5	0.03	7.2
5	0.03	11.22	0.03	11.97	0.03	12.1	0.03	12.7	0.03	13.7
10	0.13	9.09	0.13	9.4	0.13	9.8	0.13	10.3	0.13	11.3
15	0.09	10.56	0.06	11.9	0.13	13.3	0.06	11	0.06	14.1
20	0.13	10.74	0.13	11.3	0.13	11.7	0.13	11.4	0.13	12.48

Fig. 7. Comparison of drag coefficients between the baseline airfoil and the CFJ with different $C\mu$ levels at (a) $Re = 5 \cdot 10^4$, (b) $Re = 7.5 \cdot 10^4$, (c) $Re = 10^5$, (d) $Re = 1.5 \cdot 10^5$, (e) $Re = 3 \cdot 10^5$

4. Conclusion

The present study investigates the effects of the modern active flow control method over a NACA 0025 airfoil. This method was proposed by Zha and Paxton (2004) as the CFJ which included two slots of injection and suction on the suction side of the airfoil. The performance of this flow control has been numerically investigated at five Reynold numbers of $5 \cdot 10^4$, $7.5 \cdot 10^4$,
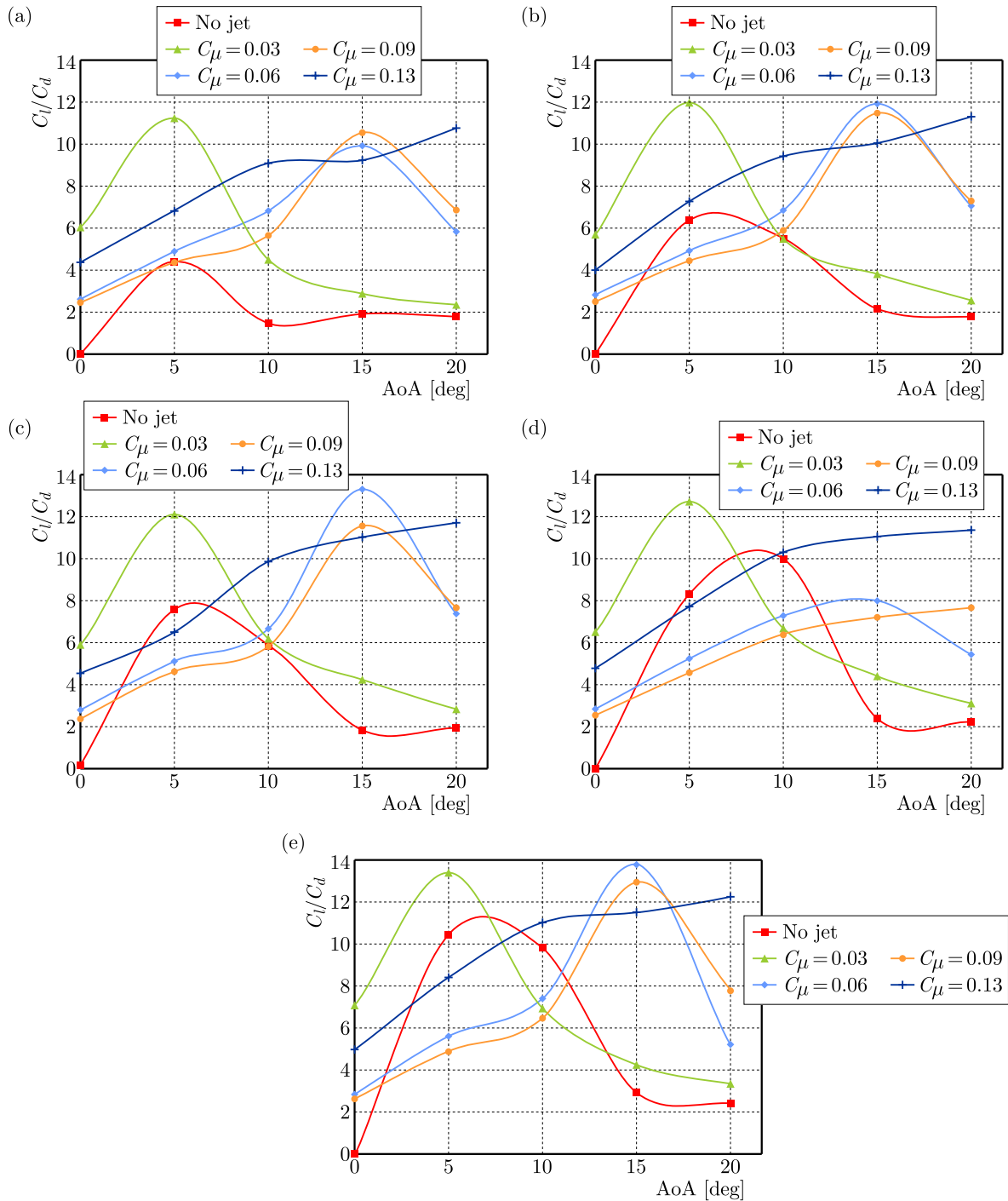
Fig. 8. Comparison of C_l/C_d between the baseline airfoil and the CFJ with different $C\mu$ levels at (a) Re $= 5 \cdot 10^4$, (b) Re $= 7.5 \cdot 10^4$, (c) Re $= 10^5$, (d) Re $= 1.5 \cdot 10^5$, (e) Re $= 3 \cdot 10^5$

10^5, $1.5 \cdot 10^5$, and $3 \cdot 10^5$ for a few momentum coefficients in the AoA range of 0° to 20°. To that end, the Reynolds-averaged Navier-Stokes equations have been solved for a 2D compressible and unsteady flow using a domestic computer program and the SST-k-ω turbulence model. The results reveal that for small angles of attack before the occurrence of stall, a small moment coefficient leads to higher efficiency and performance of the airfoil, while high values of the momentum coefficient produce inappropriate results. Therefore, there is a maximum value of the jet momentum coefficient which when exceeded decreases the system performance.

References

1. ABINAV R., NAIR N.R., SRAVAN P., KUMAR P., NAGARAJA S.R., 2016, CFD analysis of co flow jet airfoil, *Indian Journal of Science and Technology*, **9**, 45

2. DANO B., KIRK D., ZHA G., 2010, Experimental investigation of jet mixing mechanism of co-flow jet airfoil, *5th Flow Control Conference*, **AIAA 2010-4421**, Chicago, Illinois, USA

3. DANO B., ZHA G., CASTILLO M., 2011, Experimental study of co-flow jet airfoil performance enhancement using discreet jets, *49th AIAA Aerospace Sciences Meeting*, Orlando, Florida, USA

4. ETHIRAJ S., 2017, Aerodynamic performance analysis of a co-flow jet aerfoil using CFD, *International Research Journal of Engineering and Technology*, **4**, 7

5. HOSSAIN MD. A., UDDIN MD. N., ISLAM MD. R., MASHUD M., 2015, Enhancement of aerodynamic properties of an airfoil by co flow jet (CFJ) flow, *American Journal of Engineering Research*, **4**, 1

6. JANSEN K.E., RASQUIN M., FARNSWORTH J.A., RATHAY N., MONASTERO M.C., AMITAY M., 2017, Interaction of a synthetic jet with separated flow over a vertical tail, *AIAA Journal*, **56**, 7, 2653-2668

7. LEFEBVRE A., DANO B., BARTOW W.B., FRONZO M.D., ZHA G.C., 2016, Performance and energy expenditure of co-flow jet airfoil with variation of Mach number, *Journal of Aircraft*, **53**, 6, 1757-1767

8. MIRHOSSEINI M., KHOSHNEVIS A.B., 2016, Effect of adverse pressure gradient on a fluctuating velocity over the co-flow jet airfoil, *International Journal of Mechanical and Mechatronics Engineering*, **10**

9. REN Y., ZHA G., 2018, Simulation of 3D co-flow jet airfoil with embedded micro-compressor actuator, *AIAA Aerospace Sciences Meeting*, Kissimmee, Florida, USA

10. SALIMIPOUR E., SAEI MOGHADDAM M., YAZDANI S., 2016, Stall flutter control of a wing section by leading edge modifications, *Journal of Mechanical Engineering and Technology*, **8**, 1, 41-57

11. SALIMIPOUR E., YAZDANI S., 2015, Dynamic stall control of low Reynolds number airfoil with separation bubble control blade, *Modares Mechanical Engineering*, **15**, 6, 393-401

12. SALIMIPOUR E., YAZDANI S., 2020, Improvement of aerodynamic performance of an offshore wind turbine blade by moving surface mechanism, *Ocean Engineering*, **195**, 106710

13. SATYAJIT D., RATHAKRISHNAN E., 2018, Experimental study of supersonic co-flowing jet, *Proceedings of the Institution of Mechanical Engineers, Part G: Journal of Aerospace Engineering*, **233**, 4, 1237-1249

14. SHOKRGOZAR ABBASI A., YAZDANI S., 2019, A numerical investigation of synthetic jet effect on dynamic stall control of oscillating airfoil, *Scientia Iranica Articles*, DOI: 10.24200/sci.2019.52743.2870

15. WELLS A., CONELY C., CARROLL B., PAXTON C., ZHA G.C., 2006, Velocity field for an airfoil with co-flow jet flow control, *44th AIAA Aerospace Sciences Meeting and Exhibit*, Reno, Nevada, USA

16. YANG Y., ZHA G., 2018a, Improved delayed detached eddy simulation of super-lift coefficient of subsonic co-flow jet flow control airfoil, *AIAA Aerospace Sciences Meeting*, Kissimmee, Florida, USA

17. YANG Y., ZHA G., 2018b, Numerical simulation of super-lift coefficient of co-flow jet flow control wing, *AIAA Aerospace Sciences Meeting*, Kissimmee, Florida, USA

18. YARUSEVYCH S., KAWALL J.G., SULLIVAN P.E., 2006, Airfoil performance at low Reynolds numbers in the presence of periodic disturbances, *Journal of Fluids Engineering*, **128**, 3, 587

19. ZHA G., GAO W., 2006, Analysis of jet effects on co-flow jet airfoil performance with integrated propulsion system, *44th AIAA Aerospace Sciences Meeting*, **2**, Reno, NV, USA

20. ZHA G., PAXTON C., 2004, A novel airfoil circulation augment flow control method using co-flow jet, *2nd AIAA Flow Control Conference*, Portland, OR, USA

21. ZHA G., GAO W., PAXTON C.D., 2007, Jet effects on coflow jet airfoil performance, *AIAA Journal*, **45**, 6, 1222-1231

22. ZHA G., PAXTON C., CONLEY C.A., WELLS A., CARROLL B.F., 2006, Effect of injection slot size on the performance of coflow jet airfoil, *Journal of Aircraft*, **43**, 4, 987-995

23. ZHANG J., XU K., YANG Y., REN Y., PATEL P., ZHA G., 2018a, Aircraft control surfaces using co-flow jet active flow control airfoil, *Applied Aerodynamics Conference*, Atlanta, Georgia, USA

24. ZHANG J., XU K., YANG Y., YAN R., PATEL P., ZHA G., 2018b, Aircraft control surfaces using co-flow jet active flow control airfoil, *Applied Aerodynamics Conference*, Atlanta, Georgia, USA